Nash, D. F. T. & Ryde S. J. (2001). *Géotechnique* **51**, No. 3, 257–273

Modelling consolidation accelerated by vertical drains in soils subject to creep

D. F. T. NASH* and S. J. RYDE†

The settlement of embankments and reclamations over soft soils is frequently accelerated by the use of vertical drains. The magnitude of long-term settlement is sometimes reduced by the use of surcharge, although there is often uncertainty about how long the surcharge should be maintained to minimise creep movement. The design of vertical drains is generally based on closed-form solutions of Terzaghi's consolidation equation, and rarely takes into account non-linear stiffness and creep of the soil. In this paper a one-dimensional finite difference consolidation analysis is outlined showing how vertical and radial drainage of a multi-layer soil profile in the zone of influence of a vertical drain may be modelled. The analysis allows inclusion of a zone of peripheral smear around the drain and drain resistance, permeabilities may be varied with void ratio, and creep is modelled both during and after primary consolidation. The application of the model is illustrated with back-analysis of field data from construction of an embankment with temporary surcharge over estuarine alluvium.

KEYWORDS: clays; consolidation; creep; embankments; ground improvement; numerical modelling and analysis.

Le tassement des berges et la reconquête de sols tendre se trouvent fréquemment accélérées par l'utilisation de drains verticaux. L'ampleur du tassement à long terme est parfois réduite par l'utilisation d'une surcharge, bien qu'il existe souvent une incertitude quant à la durée de maintien de la surcharge pour minimiser le mouvement de glissement. L'étude de la forme des drains verticaux est généralement basée sur des solutions en forme fermée de l'équation de consolidation de Terzaghi et prend rarement en compte la rigidité non linéaire et le glissement du sol. Dans cette étude, nous décrivons une analyse unidimensionnelle de consolidation à différence finie, montrant comment le drainage vertical et radial d'un profil de sol à plusieurs couches dans la zone d'influence d'un drain vertical peut être mis en maquette. L'analyse tient compte de la zone de salissure périphérique autour du drain et des effets de la résistance de drain, les perméabilités pouvant être variées en fonction du taux de vide ; le glissement est mis en maquette pendant et après la consolidation primaire. L'application du modèle est illustrée par des rétro-analyses des données de terrain relevées pendant la construction d'une berge avec une surcharge temporaire sur des alluvions d'estuaire.

INTRODUCTION

Vertical drains are widely used in the construction of embankments and reclamations over compressible soils to accelerate their consolidation. Traditionally, vertical drains consisted of sand columns constructed by jetting, boring or displacement techniques, but nowadays the use of prefabricated band drains is widespread. When post-construction settlements are likely to be significant owing to lack of full pore pressure dissipation or creep it is common to attempt to reduce these by application of a temporary surcharge over critical areas. Such techniques have gained wide acceptance, and their design and application have been reviewed by several authors (for example (Johnson, 1970; Bjerrum, 1972; Jamiolkowski *et al.*, 1983; Holtz *et al.*, 1991). However, these authors acknowledged the difficulty of predicting settlement rates in soils exhibiting creep, and especially when the surcharge is removed.

The design of vertical drains is generally based on closed-form solutions of Terzaghi's consolidation equation (Terzaghi, 1943), in which the three-dimensional process of consolidation is simplified to that of one-dimensional movement arising from a combination of vertical flow and radial flow to the drain. Barron (1948) and Hansbo (1981) obtained solutions for equal strain (in which the surface displacements are constant but the applied stress is non-uniform), and Barron also considered free strain (in which the applied vertical stress at the surface remains constant and settlements are non-uniform). They also considered the important practical problems of smear around the drain and drain resistance effects.

Such solutions necessitate many simplifying assumptions, including that strains are only one-dimensional, that the vertical and radial coefficients of consolidation, c_v and c_r, remain constant during consolidation, and that the relationship between effective stress and void ratio is linear and independent of time. Terzaghi & Peck (1948) recognised that the stiffness of lightly over-consolidated clay deposits varies with stress level, and that secondary compression effects increase the settlements in the long term. They stated that, 'despite the radical simplifications involved, the theory of consolidation serves a useful purpose, since it permits at least a rough estimate of the rate of settlement due to consolidation, on the basis of laboratory tests'. Since then engineers have generally estimated settlement rates during primary consolidation on the basis of Terzaghi's theory (and later developments), adding on an allowance for subsequent secondary settlements. The advent of computers has enabled development of numerical methods for the analysis of consolidation. Such methods provide greater flexiblity than closed-form solutions, and permit the inclusion of a multi-layer profile including soils whose behaviour differs from that assumed by Terzaghi.

The authors recently undertook the back-analysis of field data from construction of the approach motorways to the new Second Severn Crossing in the UK, a project involving numerous embankments constructed in stages over estuarine alluvium. Previous motorway embankments in the area had exhibited large and ongoing secondary settlements. One of the objectives of this research was to examine the application of a state-of-the-art constitutive model in the back-analysis of real engineering data. In reviewing possible methods of settlement analysis, several numerical procedures were identified, but none was readily available that could model creep effects during primary consolidation. Accordingly a finite difference analysis was developed by Ryde (1997), to model one-dimensional consolidation arising from vertical and radial flow, incorporating an elastic visco-plastic constitutive model developed recently by Yin & Graham (1989, 1996). This finite strain analysis includes the effects of non-linear stiffness, creep, and permeability varying with void ratio as well as drain resistance and smear around the vertical drain. In this paper the finite difference algorithm is outlined,

Manuscript received 14 June 2000; revised manuscript accepted 11 December 2000.
Discussion on this paper closes 2 October 2001, for further details see inside back cover.
* Department of Civil Engineering, University of Bristol, UK.
†Scott Wilson Kirkpatrick and Co. Ltd, UK. Formerly Department of Civil Engineering, University of Bristol, UK.

and the way in which creep is incorporated is described. Its application in back-analysis of data from one of the new embankments is presented by way of illustration.

CREEP MODEL

Background

The first theory of secondary compression was formulated by Taylor & Merchant (1940), and since then straining under constant effective stresses has been an area of continual study. They showed that secondary compression movements decrease logarithmically with time, and Taylor (1948) stated that creep occurs during primary consolidation as well as subsequently. Following Taylor's ideas, Suklje (1957) and Bjerrum (1967, 1972) presented diagrams showing a system of approximately parallel curves of e against $\log \sigma'$ (Fig. 1) that describe secondary compression behaviour. In this widely used diagram, the lines indicate void ratio after constant time for delayed compression, or sometimes indicate constant strain rate (isotaches). Bjerrum introduced the terms *instant* and *delayed* compression to describe the behaviour of the soil skeleton in the absence of pore pressure effects, and argued that delayed compression (or creep) occurs during the whole consolidation process. Bjerrum (1972) drew attention to the significance of secondary compression for the design of vertical drain installations. He showed that although improved drainage accelerates primary consolidation, it does not affect the magnitude of total long-term settlement. He also discussed the use of temporary surcharge to reduce long-term movements.

Creep at constant effective stress is usually described using the secondary compression index $C_\alpha = \Delta e / \Delta \log t$ but there has always been a difficulty in deciding the time origin. The main area of debate (Ladd *et al.*, 1976; Jamiolkowski *et al.*, 1983; Mesri & Choi, 1985a; Leroueil, 1988) has been whether creep is significant during primary consolidation. If creep commences only after primary consolidation is complete (hypothesis A), the end of primary (EOP) e against $\log \sigma'$ curve is practically independent of the thickness of the compressible stratum and the duration of primary consolidation. If creep is significant both during and after primary compression (hypothesis B), field and laboratory stress–strain behaviour will be different.

Mesri & Choi (1985b) developed the finite difference proce-

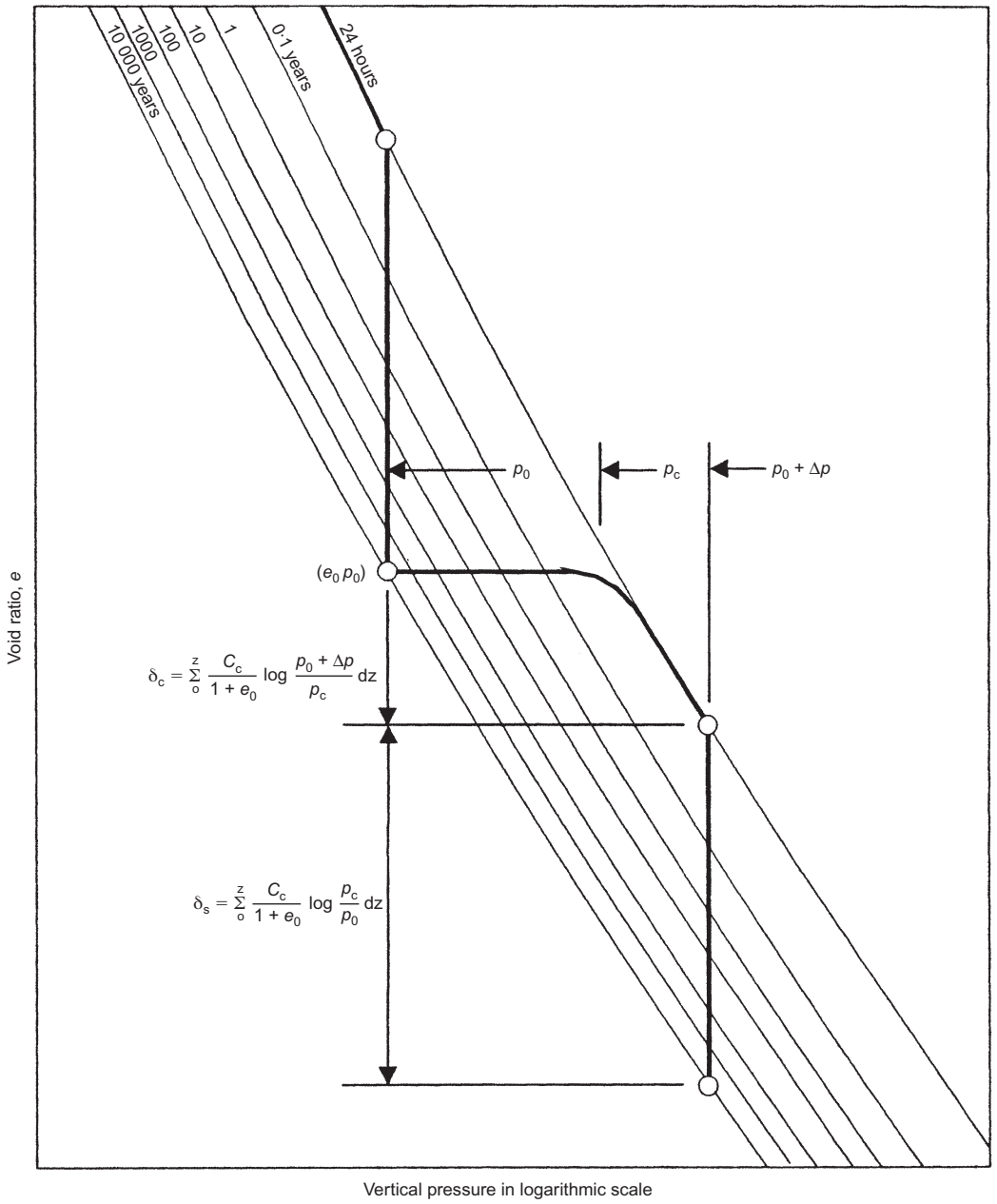

Fig. 1. Principle for evaluating secondary settlements in soft clay (Bjerrum, 1972)

dure ILLICON, which utilises hypothesis A, and the assumption is made that the secondary compression index, C_α, is linearly related to the compression index, C_c (Mesri & Godlewski, 1977). Subsequently ILLICON was extended to include flow into a vertical drain, and experience of its use was summarised by Mesri *et al.* (1994).

Bjerrum's ideas (hypothesis B) were expressed mathematically by Garlanger (1972), and Magnan *et al.* (1979) used a stress–strain–strain rate model in the one-dimensional consolidation analysis CONMULT. Kabbaj *et al.* (1986) proposed separating elastic and plastic components of strain, and subsequently Yin & Graham (1989) and Den Haan (1996) developed similar elastic visco-plastic (EVP) models that overcome previous limitations. While these EVP models have been used successfully in modelling laboratory data, there is little published on their application to full-scale problems. In selecting a model for use in back-analysis involving vertical drains, the authors concluded that it was logical to include creep during primary consolidation (hypothesis B), and desirable to be able to model creep after unloading. The EVP model of Yin & Graham was therefore adopted for this work.

Simple isotache model for one-dimensional compression

The elastic visco-plastic (EVP) model is summarised here, and the reader is referred to Yin & Graham (1989, 1994, 1996) for a fuller description. Yin & Graham used the λ–κ model from critical state soil mechanics to define the elastic–plastic behaviour of the soil skeleton, with the normal consolidation line (NCL) replaced by a reference time line (RTL), as illustrated in Fig. 2. On this diagram the parallel lines or isotaches connect soil states at which the creep strain rate is constant. One isotache on which the creep strain rate is known is chosen as the RTL, which is used to define the complete set of isotaches; equally spaced isotaches indicate a logarithmic change in strain rate. Although a lower limit to creep is observed in practice, particularly on unloading, it is not included in this simple isotache model.

The solid line ABD in Fig. 2 indicates a path that might be followed by an element of soil loaded by an instantaneous increment of total stress $\Delta\sigma$ as it consolidates. As the effective stress increases from the initial state at point A, the creep strain rate increases as the soil state moves towards the RTL, but the effective stress and strain rate are limited by the ability of the pore water to escape. After further consolidation the strain rate decreases until excess pore pressures have dissipated at point B, after which creep continues at decreasing rates towards point D. It is important to realise that the stress–strain behaviour of each element in the ground during primary consolidation will be different depending on its proximity to a drainage boundary. A soil element remote from a drainage boundary may follow the path AB indicated by the solid line, while another element closer to the drainage boundary may consolidate faster, with the path from A to B lying closer to the RTL as shown by the dashed line. For this element the end of primary consolidation occurs at point C. Indeed a small sample of the soil subjected to the same loading in an oedometer might follow a path that crossed the RTL.

The RTL is fixed by the stress[1] $\sigma_0'^{ep}$ and strain ε_0^{ep} at reference point O (see Fig. 2). The equation of the RTL is given by

$$\varepsilon^{ep} = \varepsilon_0^{ep} + \frac{\lambda}{\nu_0} \ln\left(\frac{\sigma'}{\sigma_0'^{ep}}\right) \tag{1}$$

where λ/ν_0 is its slope, and ν_0 is the specific volume at zero strain. Alternatively the equivalent expression in terms of void ratio may be used.

The incremental total strain $d\varepsilon$ resulting from a change of

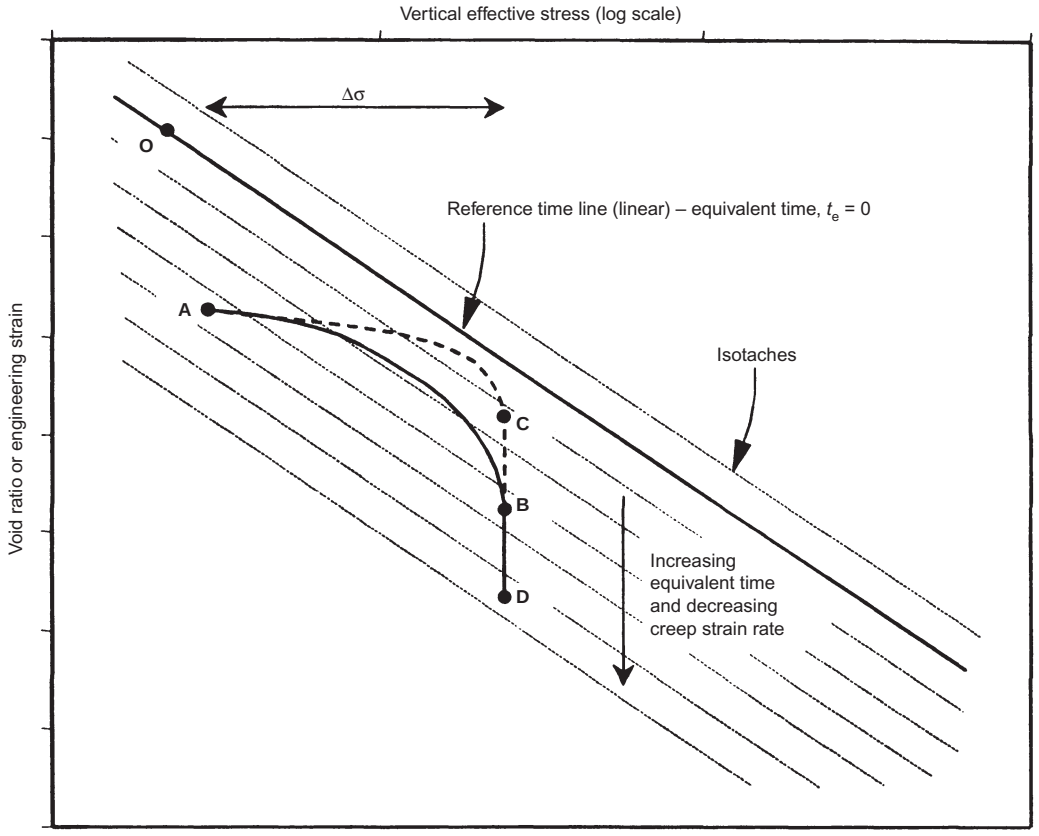

Fig. 2. Elastic visco-plastic constitutive model showing isotaches and stress–strain path during compression

[1] The superscripts *e*, *ep* and *tp* denote instantaneous (elastic), stress-dependent plastic and time-dependent plastic, respectively.

vertical effective stress $d\sigma'$ is the sum of the incremental elastic strain $d\varepsilon^{e}$ and the incremental creep strain $d\varepsilon^{tp}$ given by

$$d\varepsilon = d\varepsilon^{e} + d\varepsilon^{tp} = \frac{\kappa}{\nu_0 \sigma'} d\sigma' + d\varepsilon^{tp} \tag{2}$$

where σ' is the current vertical effective stress, and κ is the slope of the elastic unload–reload line (void ratio e against $\ln \sigma'$). The creep strain rate is defined by the relation of the current soil state to the RTL. Yin & Graham (1989) introduced the concept of equivalent time t_e, which is equal to the real time that would be taken to creep under constant effective stress from the RTL to the present state. On the RTL the equivalent time t_e is zero, and the creep strain rate is defined *a priori* using a constant t_0. The creep strain rate at other states is calculated from the expression

$$\dot{\varepsilon}^{tp} = \frac{\partial \varepsilon^{tp}}{\partial t} = \frac{\psi}{\nu_0 (t_0 + t_e)} \tag{3}$$

in which ψ/ν_0 is the slope of a plot of creep strain ε^{tp} against $\ln(t_e)$ (similar to the conventional coefficient of secondary consolidation, C_α). Thus the parallel isotaches in Fig. 2 are also t_e isochrones. It is easier to understand the model if the chosen RTL is located above the NCL, but this is not a requirement as t_e may assume negative values provided that $t_e > -t_0$.

It follows by integration of equation (3) that the difference in strain between the current state and that on the RTL at the same stress is given by

$$\Delta \varepsilon^{tp} = \frac{\psi}{\nu_0} \ln\left(1 + \frac{t_e}{t_0}\right) \tag{4}$$

and when this expression is combined with equation (1) for the RTL, the total strain is given by

$$\varepsilon = \varepsilon_0^{ep} + \frac{\lambda}{\nu_0} \ln\left(\frac{\sigma'}{\sigma_0'^{ep}}\right) + \frac{\psi}{\nu_0} \ln\left(1 + \frac{t_e}{t_0}\right) \tag{5}$$

This expression can be rearranged so that the equivalent time may be calculated from

$$t_e = -t_0 + t_0 \exp\left[(\varepsilon - \varepsilon_0^{ep}) \frac{\nu_0}{\psi}\right] \times \left(\frac{\sigma'}{\sigma_0'^{ep}}\right)^{-\lambda/\psi} \tag{6}$$

The model parameters may be obtained from high-quality incremental load oedometer tests. The RTL is first located on a plot of void ratio or engineering strain against $\log \sigma'$, passing through points of constant creep strain rate, approximately parallel to the normal consolidation line. Yin & Graham (1994) suggest an iterative procedure to locate the RTL above the NCL, particularly when load increments are applied after variable time intervals. However, the authors have found that in many oedometer tests with increments applied daily, the strain rate after 24 hours is approximately constant in the normally consolidated stress range. The 24 hour line may then be used directly as the RTL, and its position defined by projecting it back to the zero strain axis, taking the intercept to be the stress $\sigma_0'^{ep}$ and setting $\varepsilon_0^{ep} = 0$. Values of λ and κ are found from the slopes of the chosen RTL and the unloading/reloading curves, and the remaining parameters are found from the creep data. By combining equations (3) and (4) it follows that when the soil creeps at constant effective stress:

$$\varepsilon^{tp} = \psi/\nu_0 \left[\ln\left(\frac{\psi}{\nu_0 t_0}\right) - \ln(\dot{\varepsilon}^{tp})\right] \tag{7}$$

The parameter ψ or the combination ψ/ν_0 may readily be obtained from the slope of plots of logarithm of strain rate against strain for the later stages of each increment (Nash & Ryde, 2000). The value of t_0 is then calculated from the creep rate on the RTL.

The EVP model used here is formulated in terms of engineering strain and assumes a linear RTL on a plot of void ratio (or engineering strain) against $\log \sigma'$, but this is not a requirement. Many structured clays exhibit non-linear normal consolidation lines, and recently Nash & Ryde (2000) have extended this EVP model to include a curved RTL using natural strain (after Butterfield, 1979) or a power law (after Den Haan, 1992).

CONSOLIDATION EQUATION

The axisymmetric form of the one-dimensional consolidation equation (Terzaghi, 1943) is often written

$$c_v \frac{\partial^2 \bar{u}}{\partial z^2} + c_r \left(\frac{\partial^2 \bar{u}}{\partial r^2} + \frac{1}{r}\frac{\partial \bar{u}}{\partial r}\right) = \frac{\partial \bar{u}}{\partial t} \tag{8}$$

in which $\bar{u}$ is the excess pore pressure, and c_v and c_r are the vertical and radial coefficients of consolidation respectively. In derivation of this equation for a small element of soil, it is assumed that strain is one-dimensional in the vertical direction, but that flow may be vertical and radial. Furthermore it is assumed that the principal axes of permeability coincide with the vertical and radial directions, an assumption that is consistent with a horizontally layered soil.

Terzaghi (1943) discusses the application of solutions of equation (8) to a practical problem involving vertical drains. Each vertical drain is considered to be located at the centre of a cylinder of soil of external diameter approximately equal to the drain spacing, and with interior diameter equal to that of the drain. Drainage may occur at the permeable inner boundary and at the top and/or bottom surfaces. Terzaghi uses the work of Carrillo (1942) to show how the principle of superposition may be used to combine the theoretical solutions for separate radial and vertical flow problems. Similar procedures were adopted by Barron (1948) and Hansbo (1981). Such solutions to the consolidation equation necessitate a number of assumptions, including constant applied load during consolidation, constant coefficients of consolidation, deformations that are small compared with the original geometry and are one-dimensional, and constant boundary pore-pressure conditions. These assumptions are not valid for the consolidation of thick layers of soft clay in which a large proportion of the compression is due to creep, and closed-form solutions are not available.

The consolidation equation is generally expressed in terms of excess pore pressure, $\bar{u}$, on the assumption that the steady-state pore pressure, u_{ss}, remains constant. The terms involving $\bar{u}$ are derived from total head h and position head z, where

$$h = \frac{u}{\gamma_w} + z = \frac{\bar{u} + u_{ss}}{\gamma_w} + z \tag{9}$$

If the boundary conditions may change, it is convenient to use the full pore pressure u, with an additional term on the left-hand side of the consolidation equation to account for the variation of pressure with elevation. If there is spatial variation of permeabilities k_z and k_r in vertical and radial directions it is necessary to include them within each derivative in equation (8), which may then be written

$$\frac{\partial}{\partial z}\left[\frac{k_z}{\gamma_w}\left(\frac{\partial u}{\partial z} + \gamma_w\right)\right] + \frac{1}{r}\frac{\partial}{\partial r}\left[\frac{k_r}{\gamma_w} r \frac{\partial u}{\partial r}\right] = m_v \left(\frac{\partial u}{\partial t} - \frac{\partial \sigma}{\partial t}\right) + \frac{\partial \varepsilon^{tp}}{\partial t} \tag{10}$$

where m_v is the coefficient of volume compressibility. The variation of total vertical stress elastic σ with time, and creep are taken into account by inclusion of additional terms on the right-hand side, which expresses the elastic and plastic components of strain rate. If the boundary pore pressures do not change, the equation may be expressed in terms of excess pore pressure $\bar{u}$, and the extra term involving γ_w is omitted. The soil may be modelled as linear elastic (using a constant m_v) or non-linear (by varying m_v with stress level), with or without creep. The EVP model outlined above is expressed in terms of engineering strain, and was implemented by Yin & Graham

(1996) in a small-strain formulation of the consolidation equation. When applied to large-strain problems it is necessary to allow for the change of geometry, and the strains on the right-hand side of equation (10) must be expressed as natural strains. This is achieved by multiplying the expressions in equation (2) by the ratio v_0/v, where v is the current specific volume.

Finite difference formulation

In order to model the consolidation of layered soil profiles due to vertical and radial flow, equation (10) has been expressed in finite difference form (Ryde 1997).[2] The use of finite difference methods for the analysis of consolidation problems is well established in the geotechnical literature (e.g. Richart, 1959; Murray, 1971; Olsen *et al.*, 1974; Lee *et al.*, 1983; Onoue, 1988). However, Ryde (1997) adopted a numerical formulation technique different from that previously used, similar to that developed by Reece (1986) in the analysis of heat flow through a non-uniform metal bar. The soil is divided into a series of layers and annuli, as shown in Fig. 3. The grid is graded in both directions so that there are small layer and annulus thicknesses close to permeable boundaries. The state of the soil in each cell is represented by the conditions at a central node, which is positioned so that the cell boundaries lie midway between adjacent nodes. Phantom nodes and layers are placed just outside the boundaries of the grid to enable the boundary conditions to be defined. This contrasts with previous consolidation analyses in which the nodes were generally positioned at the cell boundaries.

Figure 4 shows part of the grid in the vicinity of a cell with a central node at coordinates $r_{i,j}$ and $z_{i,j}$. For this cell the left-hand side of equation (10) may be expressed in finite difference form:

$$\frac{\dfrac{k_T}{\gamma_w}\left(\dfrac{u^*_{i,j+1}-u^*_{i,j}}{z_{i,j+1}-z_{i,j}}+\gamma_w\right)-\dfrac{k_B}{\gamma_w}\left(\dfrac{u^*_{i,j}-u^*_{i,j-1}}{z_{i,j}-z_{i,j-1}}+\gamma_w\right)}{z_T-z_B} + \frac{1}{r_{i,j}}\frac{\dfrac{k_o}{\gamma_w}r_o\left(\dfrac{u^*_{i+1,j}-u^*_{i,j}}{r_{i+1,j}-r_{i,j}}\right)-\dfrac{k_I}{\gamma_w}r_I\left(\dfrac{u^*_{i,j}-u^*_{i,j-1}}{r_{i,j}-r_{i,j-1}}\right)}{r_o-r_I} \tag{11}$$

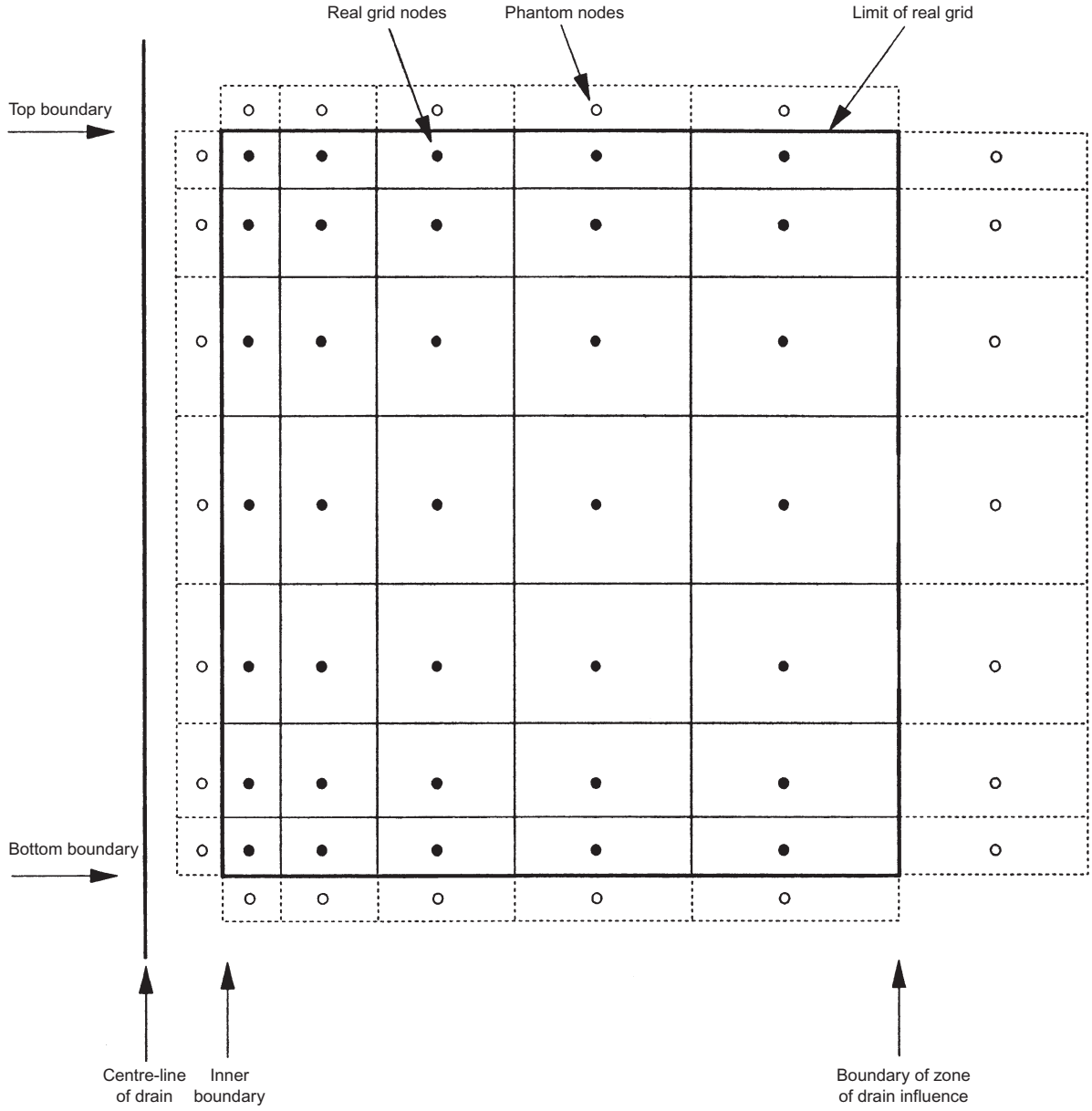

Fig. 3. Grid used in finite difference analysis

[2] Originally, Ryde (1997) formulated equation (10) in terms of excess pore pressure not full pore pressure.

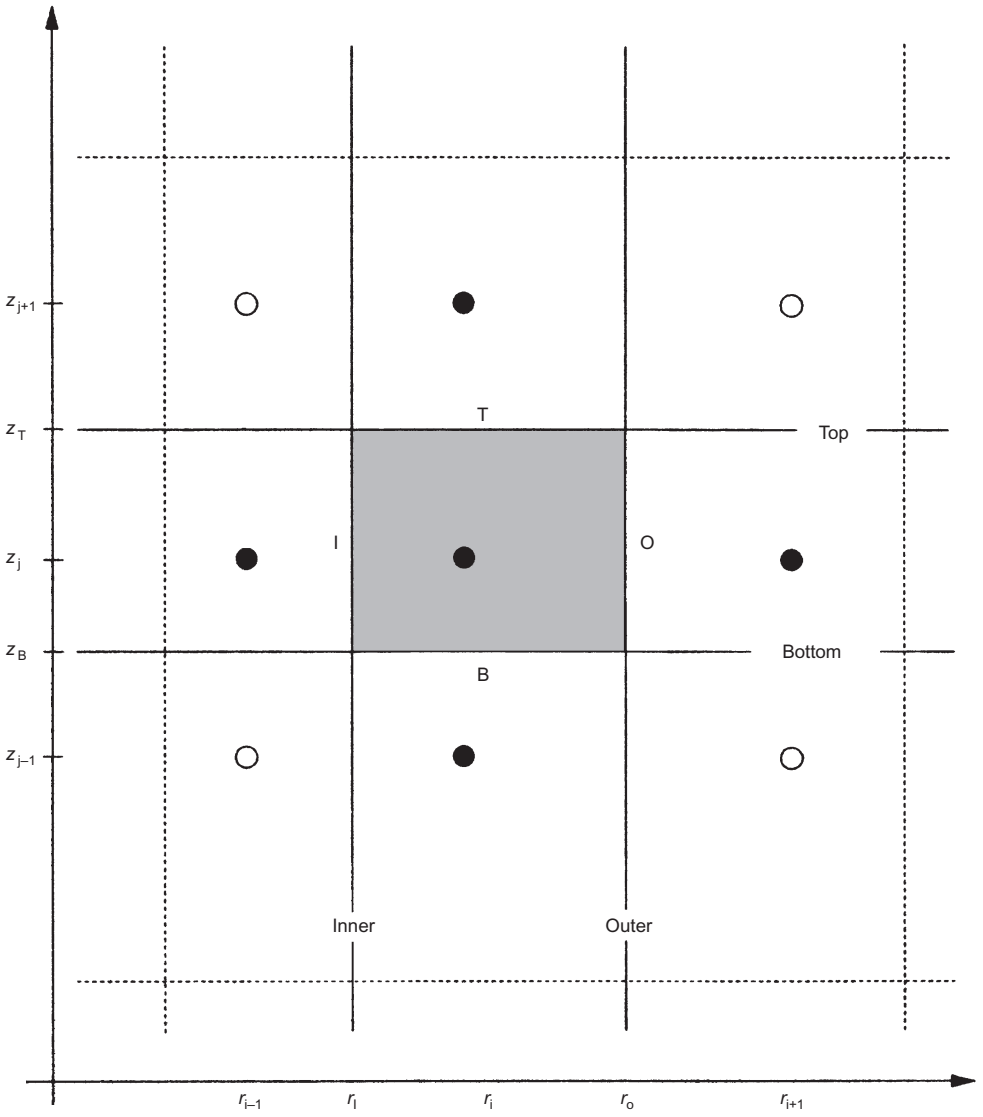

Fig. 4. Part of finite difference grid in vicinity of node *ij*

where u^* are values of the pore pressure at the central node and the nodes in the surrounding cells, and k_T etc. are the values of permeability at the boundaries between adjacent cells. Each boundary permeability is calculated from the permeabilities of the adjacent cells in the manner of:

$$k_T = \frac{2k_{i,j+1}k_{i,j}}{k_{i,j+1} + k_{i,j}} \tag{12}$$

and is applied at the cell interface to give a uniform hydraulic resistance between two adjacent nodes equivalent to the combined resistance of the two soils. This formulation has the advantage that discontinuities of permeability at layer and drainage boundaries can be handled without difficulty. It may be seen that if one soil has a very low permeability, the interface permeability is also very small, while if one soil has a very high permeability, the interface permeability is twice that of the other layer. This ensures the correct hydraulic gradient at the interface for use in equation (11). The detailed derivation of equation (12) is given in Appendix 1.

When an increment of total stress is applied, the pore pressure at depth is normally incremented by an equal amount. If appropriate, allowance may be made for the effects of reduction of applied stress with depth and partial saturation. If the total stress is only increased between small time steps, it remains constant during the time step, so the term $\partial\sigma/\partial t$ is zero. The finite difference form of the right-hand side of equation (10) may then be expressed as

$$m_v \frac{u_{i,j,t+\Delta t} - u_{i,j,t}}{\Delta t} + \dot{\varepsilon}^{tp*} \tag{13}$$

Here the first term is the elastic component of strain during the time step Δt and the second is the average creep strain rate. For each soil element, knowing the soil state (effective stress and void ratio) at any time, values of elastic compressibility and creep strain rate are determined using the constitutive model.

Boundary conditions

As noted above, phantom nodes are introduced outside the grid, as shown in Fig. 3. At a permeable boundary the pore pressure at each phantom node is set to the appropriate value, and the permeability of the phantom cell is set to a very high number. At an impermeable boundary, the permeability of each phantom cell is set to zero, resulting in zero interface permeability calculated with equation (12). This results in a zero term in equation (11), equivalent to setting the hydraulic gradient to zero.

While free drainage is normally assumed at the vertical drain, the effects of drain resistance may be modelled explicitly by incorporating the drain within the grid. The drain annulus is given equivalent discharge capacity and an impermeable core,

and the terms on the right-hand side of equation (10) for the relevant cells are set to equal zero.

Solution procedure

The terms in the finite difference equation marked with a * are used to predict the pore pressures at the end of the time step. In an explicit finite difference formulation, u^* are the values of pore pressure u_t at the *start* of the time step that are known, which enables a solution to be achieved without iteration. However, despite the simplicity of an explicit formulation, very small time steps have to be used to ensure numerical stability. In an implicit formulation the values u^* include the values $u_{t+\Delta t}$ at the *end* of the time step, which *a priori* are unknown, and for two-dimensional problems this necessitates integration. Ryde (1997) used a fully implicit formulation, and more recently the procedure has been extended to permit use of the form proposed by Crank & Nicolson (1947), where u^* is given by

$$u^* = (u_t + u_{t+\Delta t})/2 \tag{14}$$

In both forms, the creep strain is calculated from the average of the creep rates at the start and end of each time step.

By adopting a procedure of elimination and back-substitution using the Thomas algorithm or tri-diagonal matrix algorithm (TDMA), described for example by Morton & Mayers (1994), a solution is obtained efficiently. For one-dimensional problems without creep, no iteration is required, but for more complicated problems several iterations are needed at each time step. It is found that with the implicit formulation, which is inherently numerically stable, variable time steps may be used with small steps specified when strain rates are highest to achieve satisfactory accuracy. Using the Crank–Nicolson formulation similar results are obtained, but smaller steps are required when modelling creep to prevent numerical instability, while the explicit form requires very small steps. The solution has been implemented in a procedure termed BRISCON using Visual Basic for Excel, with data held on worksheets, permitting graphs to be plotted conveniently. The schematic solution algorithm is shown in Fig. 5.

At the start of the analysis the steady-state conditions are determined by iteration with the right-hand side of equation (10) set to zero. These pore pressures are used to determine the initial distribution of effective stress. As the analysis proceeds the coordinates may be updated, with the values of soil bulk density, permeability, stiffness and creep rate being those applicable to the current soil state. With increasing settlement the applied loading may change owing to partial submergence of the fill, and also the boundary conditions change as noted by Olsen & Ladd (1979). By updating the boundary pore pressures during the analysis this effect is taken into account, since the pore pressures obtained in the solution converge to the long-term steady-state values.

Free strain and equal strain solutions

The analysis described here is not a fully coupled axisymmetric analysis, since although the drainage is vertical and radial, the movements are vertical. The vertical strains in adjacent annuli at any time are not necessarily compatible, and the settlement adjacent to a vertical drain may be significantly larger than that midway between the drains. To simulate an equal strain condition the total stresses applied at ground level may be redistributed. Corrective loads are applied to the top of each annulus to maintain the surface horizontal within a specified tolerance as the analysis proceeds, and this requires additional iteration at each time step. The average settlement at any time is calculated from the settlement of each annulus using an area-weighting procedure. As expected, the difference of average settlement between the free and equal strain solutions is generally not of engineering significance, and for most analyses the extra solution time for the latter is generally not justified.

VALIDATION

During development, BRISCON was used to analyse some simple problems, and where possible comparison was made with closed-form solutions and also with solutions obtained using the finite element program CRISP (Ryde, 1997). Implementation of the creep model was checked by making comparison with problems analysed by Yin & Graham (1996). The analyses carried out are listed in Table 1, and some of these are presented here.

Comparisons with closed-form solutions

Analyses were undertaken for comparison with closed-form solutions for consolidation with vertical flow (Terzaghi 1943), and radial flow with and without a smear zone (Barron, 1948; Hansbo, 1981). In these analyses consolidation of a 6 m thick linear-elastic soil under an applied load increment of 100 kPa was modelled. In the analyses with radial flow, the radius of the drain was 0·02 m, and that of the equivalent soil cylinder was 2 m. The coefficients of permeability of the soil in the horizontal and vertical directions were 10^{-3} and 5×10^{-4} m/day respectively. In some of the analyses a smear zone was introduced out to a radius of 0·14 m, in which the permeability was reduced by a factor of 2 to equal the vertical permeability. The coefficient of volume compressibility, m_v, was 10^{-4} m^2/kN. The grid used contained eight layers of soil with twelve annuli (four of which were for the smear zone), with the grid size in each direction increasing with distance from the drainage boundaries. The results of several of these analyses are shown in Fig. 6, where average degree of consolidation is plotted against time factor for the three cases of vertical flow only, and radial flow only with and without smear. It may be seen that the finite difference procedure yields results that are very similar to the closed-form solutions. The figure also illustrates the similarity of the BRISCON results for the fixed and free strain solutions.

Comparisons with CRISP

Comparative analyses were performed for the case of radial flow with a smear zone using the finite element program CRISP with a mesh similar to the grid used in the finite difference analysis, and identical soil properties. CRISP uses a fully coupled consolidation formulation, and the stresses at any depth in the soil are redistributed within the ground to ensure strain compatibility. A uniform loading was applied to the ground surface, and since the ground surface was not maintained horizontal the solution was expected to be intermediate between a free and fixed strain analysis. The results for the case where smear was modelled are shown in Fig. 6 alongside those using BRISCON, and indicate good agreement between the progress of consolidation predicted by the two numerical analyses.

The surface settlement profile and radial pore pressure distribution were also compared at four stages during consolidation (after 5, 20, 50 and 100 days, corresponding to time factors of 0·03, 0·06, 0·32 and 0·64). Fig. 7(a) shows that for the equal strain analysis BRISCON maintained the surface level, whereas for the free strain analysis there were large settlements immediately adjacent to the vertical drainage boundary. The settlement profiles obtained using CRISP were intermediate between the two cases, as would be expected for a material with significant shear stiffness. The excess pore pressure distributions are shown in Fig. 7(b), and a distinct change of gradient at the boundary of the smear zone may be observed. The distributions were very similar for all three analyses. This is perhaps surprising since the distribution of stresses was different, but as the average settlement rates were similar, and settlement is related directly to the rate of expulsion of water, the hydraulic gradients at any time must also be similar.

Validation of creep model

To check implementation of the creep model, BRISCON was used to repeat analyses presented by Yin & Graham (1996) of

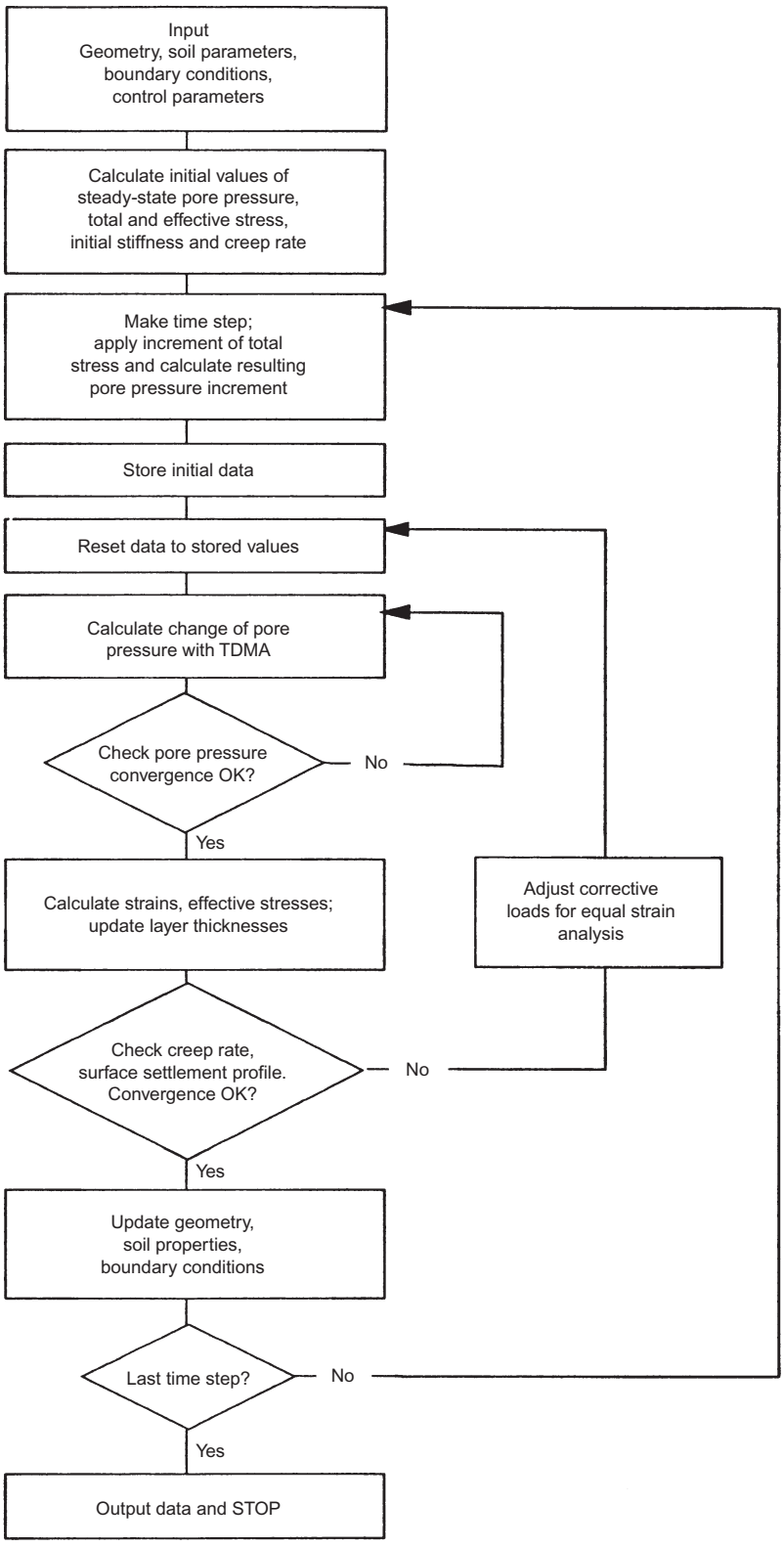

Fig. 5. Schematic algorithm for finite difference procedure BRISCON

Table 1. Analyses carried out during validation of BRISCON

Analysis	Flow direction	Soil type	Equal or free strain	Comparison with	
				CRISP	Closed form solution
1	Vertical	Linear elastic		✓	Terzaghi (1943)
2	Vertical	$\lambda\kappa$ without creep		✓	Mesri & Rokhsar (1974)
3	Vertical	$\lambda\kappa$ with creep			Yin & Graham (1996)
4	Radial	Linear elastic	Free	✓	Barron (1948)
5	Radial	Linear elastic	Equal		Barron (1948), Hansbo (1981)

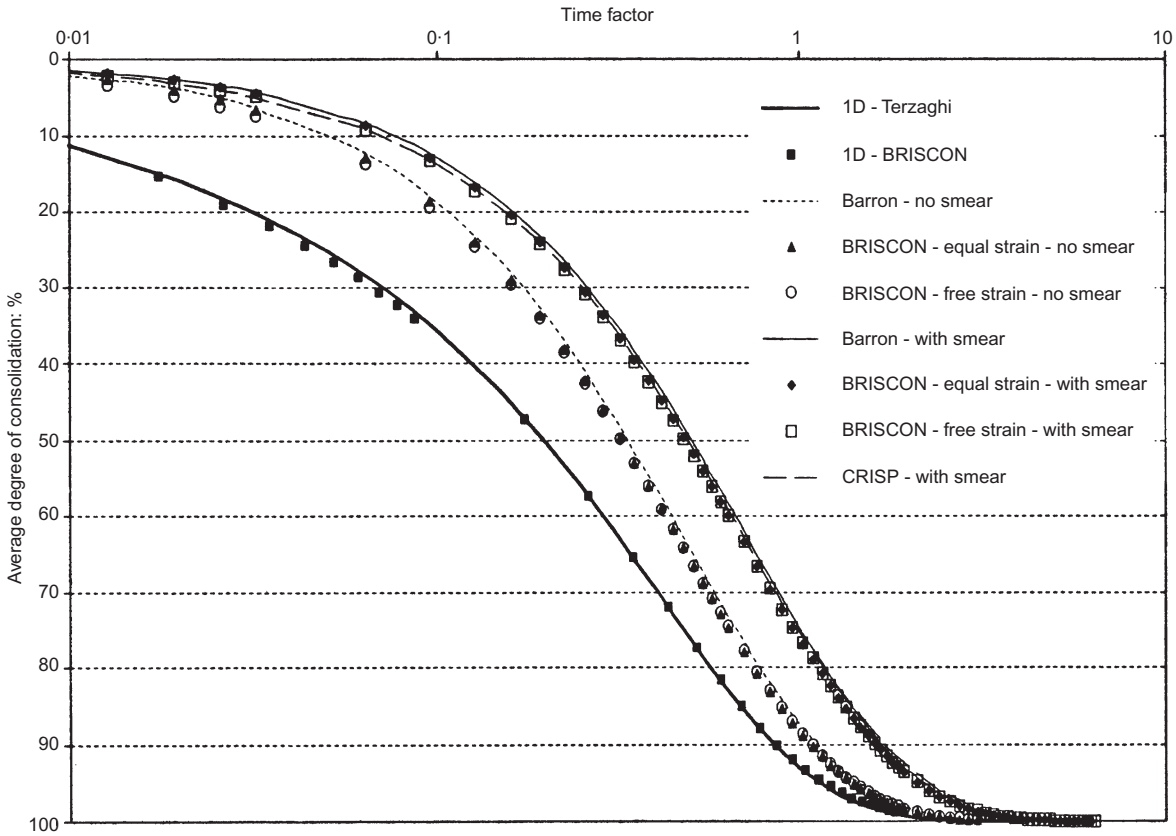

Fig. 6. Variation of average degree of consolidation with time factor in validation analyses

data from some oedometer tests on post-glacial marine clay from Drammen, Norway, published by Berre & Iversen (1972). Using identical soil/model parameters the results using BRISCON were very similar to those given by Yin & Graham (1996), which themselves provided a good fit to the laboratory data.

APPLICATION

The BRISCON procedure was developed for the back-analysis of settlement of embankments constructed as part of the new M4 and M49 approach motorways to the Second Severn Crossing, which connects England to South Wales. The 16 km length of motorways passes on low embankments across the Severnside Levels, an extensive area of estuarine alluvium bordering the estuary of the River Severn near Avonmouth, an industrial town near Bristol. Some 20 major roads, lanes and farm tracks cross the motorways on embankments typically 9 m high, which were constructed in stages and surcharged, with consolidation accelerated by vertical drains. Ideally, embankments would have been selected for particular study for which there were high-quality oedometer tests available, and class A predictions (Lambe, 1973) undertaken prior to construction followed by back-analysis of data from field monitoring. However, the variability of the estuarine alluvium coupled with insufficient good-quality laboratory data meant that only back-analysis of the field monitoring data was practicable. Accordingly the behaviour of one embankment (A403 overbridge on the M49 at Severn Beach) is described here, and the back-analysis is used to illustrate some of the features of BRISCON.

Ground conditions

The 10–20 m thick estuarine soils of the Severnside levels have a surface elevation of +6 to +7 m OD, and overlie the Mercia Mudstone bedrock. Above OD the soft silts and clays are extremely variable and often laminated with sands, and contain thin discontinuous peat bands. At depth, the strata consist of sandy sediments and terrace gravels. The silty clays are of medium to high plasticity, with undrained shear strengths of 10–30 kPa. The strata are generally lightly over-consolidated, with an OCR usually between 1·1 and 1·4. Reclamation and drainage has resulted in some groundwater lowering, with the result that the upper few metres of the soft clay are generally desiccated. Groundwater levels are controlled by lateral seepage through the granular deposits, generally varying from about +6 m OD inland to around OD at the estuary.

At the A403 overbridge the alluvium is approximately 11 m thick, as shown in the geotechnical profile in Fig. 8. The CPT profiles are shown here just for the soft clay, and indicate the heterogeneous nature of the estuarine alluvium. The alluvium is locally under-drained here, with the water table initially at 7 m depth at just below Ordnance Datum. The under-drainage arises from lateral seepage through the terrace gravel into a nearby cutting leading to a railway tunnel beneath the River Severn.

Construction

Before construction of the original M5 motorway across the Severnside levels in the 1970s, a trial embankment at Avonmouth (Murray, 1971) had shown that primary consolidation might take at least 2 years. Nevertheless the M5 was constructed without vertical drains, but in places lightweight fill was used to minimise imposed stresses. Subsequently large and ongoing settlements were reported on the M5 further south (Cook & Pereira, 1991). For the new motorways, consolidation beneath high embankments was accelerated by vertical drains, and surcharge was placed to minimise post-construction settlement.

The embankments for the A403 overbridge were constructed of Mercia Mudstone excavated from cuttings under construction elsewhere on the site. After placing a 0·6 m layer of granular fill, vertical Mebra drains were installed at 2–4 m spacing on a square grid through the compressible alluvium down into the silty sand, instrumentation was installed, and a further 0·9 m drainage layer was placed, with a geotextile separator on top.

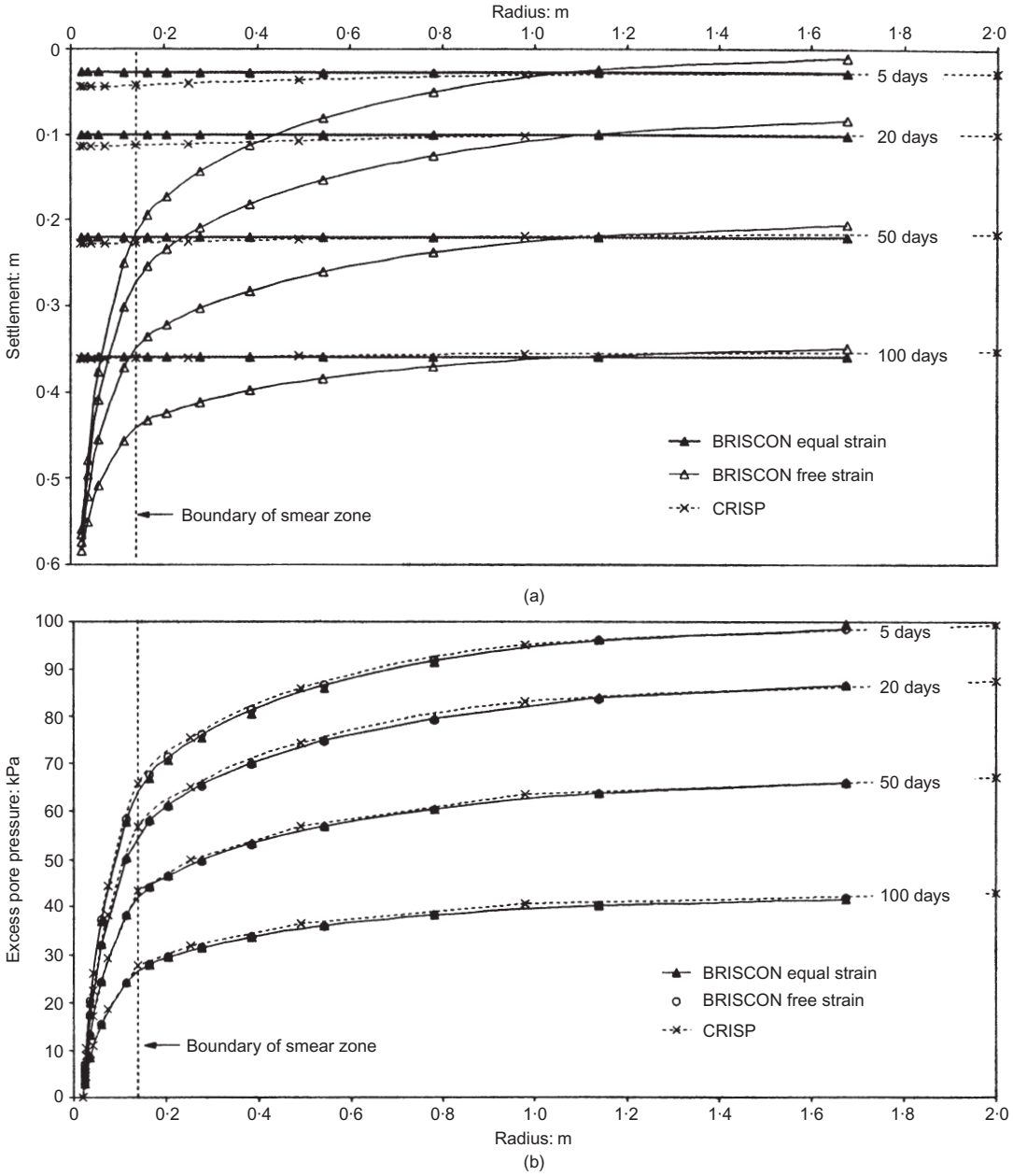

Fig. 7. Comparison of finite difference analyses (BRISCON) with finite element analysis (CRISP): (a) variation of surface settlement with radius; (b) variation of excess pore pressure with radius

After embankment construction in stages to a height of 9 m above original ground level, an extra 2 m surcharge was applied and left for 5 months. After removing the surcharge, bored piles for the bridge abutments were installed to bedrock. The finished crest width is 13 m and the side slopes are 1 in 2·5.

Observed performance of embankments

During construction of the high embankments, rod settlement gauges, magnet extensometers, inclinometers and pneumatic piezometers installed midway between vertical drains were monitored regularly to ensure embankment stability. In general, fill rates were slow and the vertical drains ensured that excess pore pressures were small, with the result that the response of the alluvium to loading was more *drained* than *undrained*.

Figure 9(a) shows the increase of maximum fill height at the A403 overbridge with time, together with the observed settlement of the original ground surface beneath the highest part of the embankment. The majority of the 700 mm settlement occurred as the fill was placed, and lateral movements (not shown here) beneath the embankment toe did not exceed 7% of the maximum settlement. It may be seen that there was a very small upward movement when the surcharge was removed, before creep settlements resumed.

Figure 9(b) shows the observations made with pneumatic piezometers beneath the centre of the embankment. Initially the pore pressures in the silty clays were small, and consistent with the under-drainage, and the piezometric levels indicated downward seepage. During the first stage of filling, when the embankment was raised to a height of 7 m over a period of 2 months, both the upper piezometers responded to the increase in vertical stress, but the response was small with maximum excess pore pressures of around 25 kPa ($\Delta u/\Delta\sigma \approx 0{\cdot}2$). The piezometric levels reduced almost immediately, and there was no further response 1 month later when the embankment was raised to its full height of just over 11 m (including surcharge). The pair of piezometers in the lower alluvium and underlying sand showed negligible response to filling, but there was a marked rise in pore pressures some time after the surcharge was placed. This appears to be unrelated to consolidation, since it affected the sand layer as well as the overlying clay, but it did occur after a period of heavy rain. By this time the original ground surface beneath the

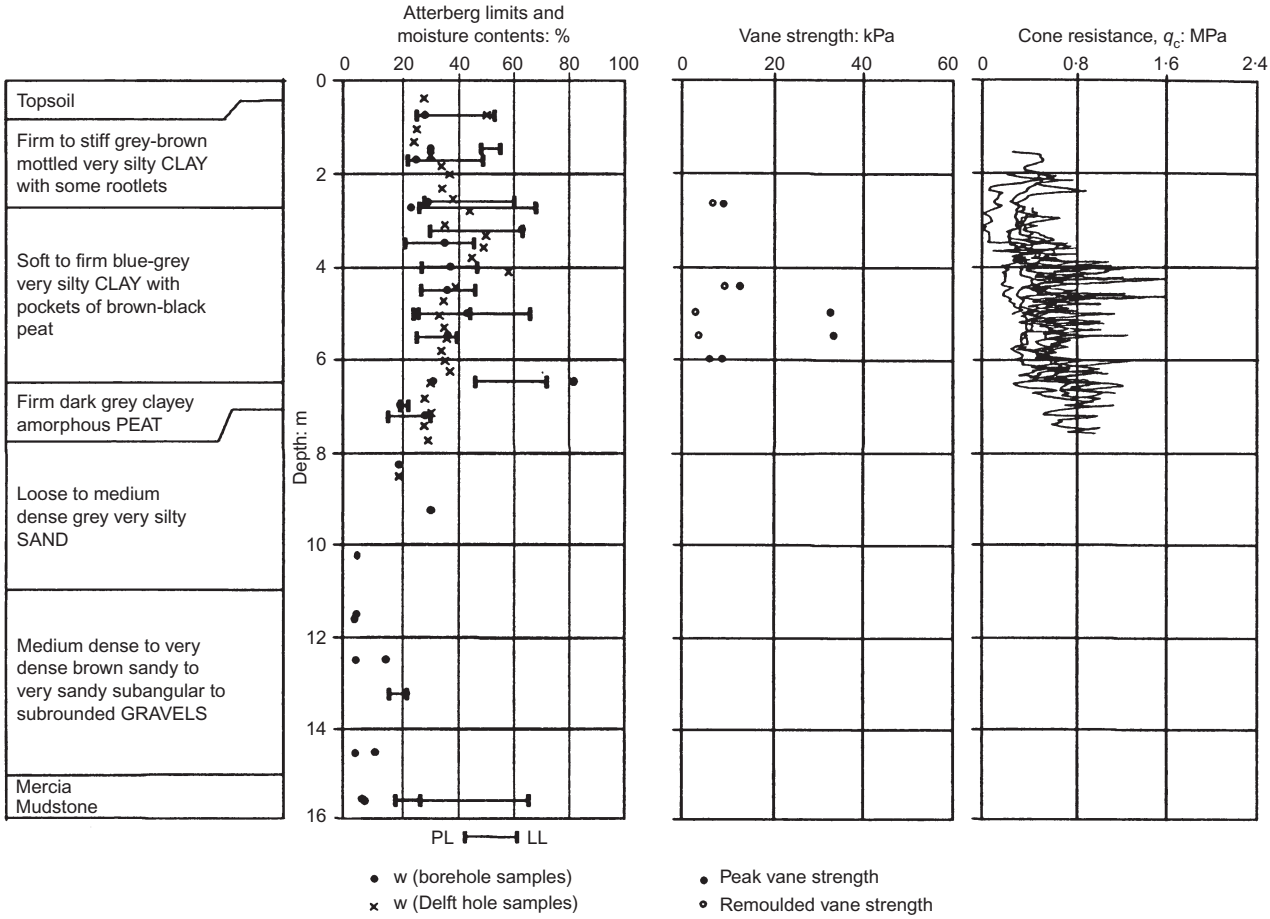

Fig. 8. Geotechnical profile at A403 overbridge on M49

embankment had settled by 600 mm, so that surface runoff (see Fig. 9(b)) may have ponded in the granular drainage layer beneath the fill. The water would then have entered the top of the vertical drains, draining into the alluvium at depth and temporarily raising the pore pressures.

Back-analysis

Back-analysis of the behaviour of this embankment was undertaken using BRISCON. Although the groundwater conditions were different from those elsewhere, this embankment was chosen because of the reliability of the instrumentation data. Since there were insufficient lab test data from this location to obtain reliable consolidation parameters, the modelling was based on the stress–strain behaviour in the field determined from piezometer and extensometer data. The profile was split into layers based on the extensometer magnet elevations: firm crust (0–3 m depth), soft silty clay and peat (3–7 m) and silty clay and sand (7–11 m); below 11 m the extensometers showed the strata to be incompressible.

Starting from the initial conditions, the average void ratio was determined for each clay layer for each stage of construction. The proportions of the embankment and underlying alluvium were such that the stress increment was reasonably uniform with depth, so that the vertical effective stress at the centre of each layer could be calculated using fill thickness and nearby piezometer data. The average void ratio could then be related to average vertical effective stress, as shown in Fig. 10.

The small strains under the first 60 kPa of the applied loading suggest that the strata were initially over-consolidated. Such behaviour was not generally observed elsewhere on this project, and was probably associated with the under-drainage. With the water table drawn down to 7 m depth comparatively recently, it might be expected that the OCR would be around 1·0. Although piezometers indicated small positive pore pressures in the clay at the start of construction, suctions developed during dry periods in the past would have left the clay over-consolidated. For the later stages of construction under high embankment loading these strata appear normally consolidated, and field normal consolidation lines (NCL) were drawn as indicated in Fig. 10, enabling average λ and κ parameters to be determined for each clay layer.

Reference time lines (RTL) for each layer were initially chosen parallel to each NCL. During construction there were two significant rest periods after fill lifts, and once excess pore pressures had dissipated there was creep at constant effective stress (see Fig. 10). Working with plots of average void ratio against $\log(t)$ for these rest periods, Ryde (1997) optimised the position of each RTL using an iterative procedure similar to Yin & Graham (1994), and determined the remaining creep parameters ψ and t_0. The full set of parameters together with m_v derived for the silty sand layer are given in Table 2. The ratio ψ/λ is around 0·1, somewhat higher than would normally be expected for the similar ratio C_α/C_c, and this is thought to be due to the presence of minor peat bands within the alluvium.

Recently the values of ψ have been confirmed by re-plotting the data in the form logarithm of strain rate against strain, as suggested by equation (7). Fig. 11 indicates reasonably linear and parallel data for each layer for the two rest periods. Two pairs of parallel lines with gradients ψ/ν_0 equal to 0·0065 and 0·0116 obtained from Table 2 for the crust and soft clay respectively have been superimposed on the data, and may be seen to fit the field data satisfactorily. This procedure appears to be more straightforward than the iterative method originally used.

Analyses with BRISCON

The analyses with BRISCON were carried out for a soil cylinder of radius 1 m with a central drain of radius of 0·033 m.

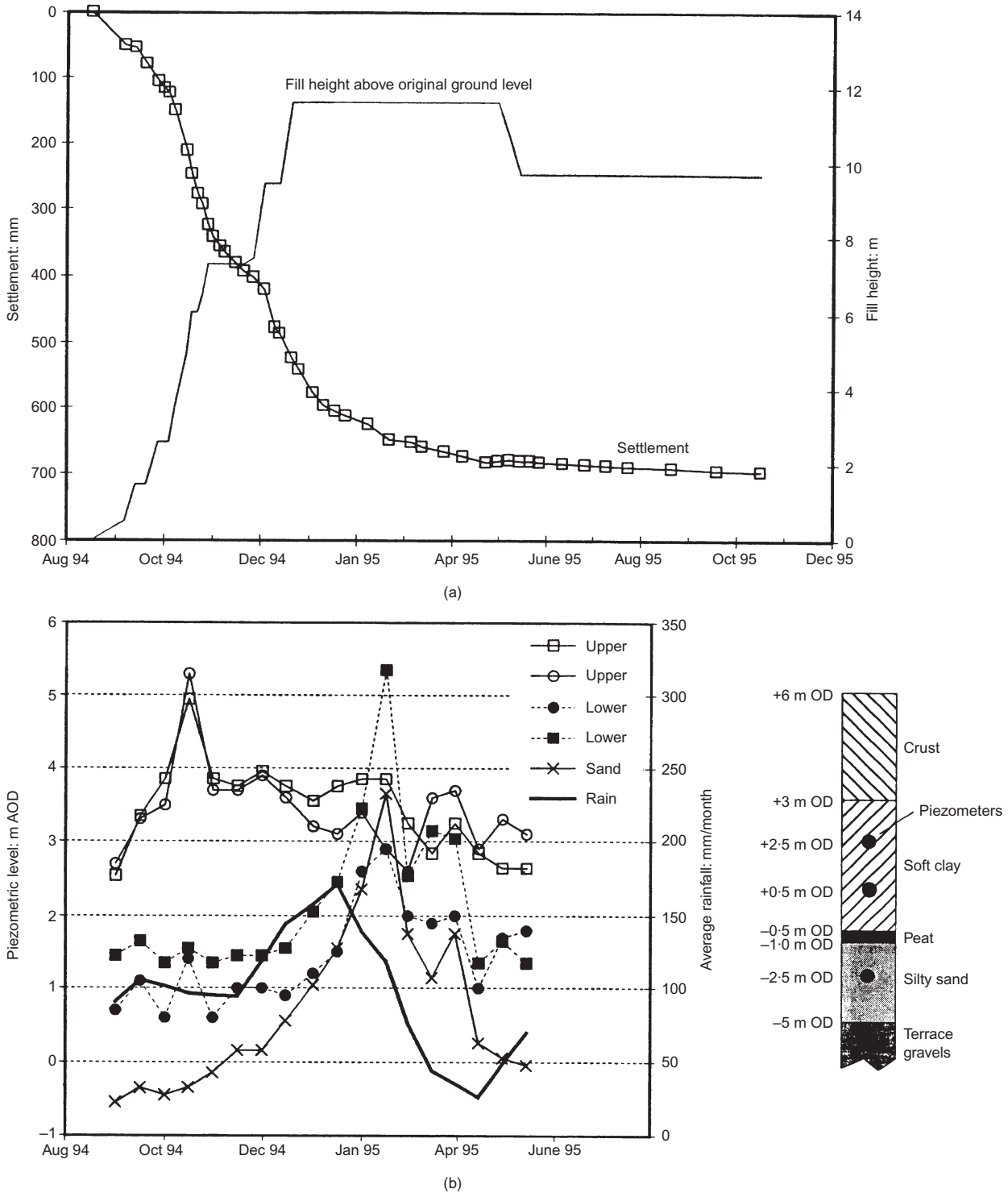

Fig. 9. Settlement and pore pressures observed during construction of A403 overbridge embankment

This configuration was approximately equivalent to Mebra drains of cross-section 100 mm by 3 mm spaced at 2 m on a square grid; the perimeter of the circular drain modelled was set equal to that of the rectangular vertical drain. The analysis used a finite difference grid of 14 layers and 6 annuli. There were few definitive data on the in-situ permeability at the A403 site, and reference was made to the report on the Avonmouth trial embankment (Murray, 1971), from which values of in-situ horizontal permeability of $1{\cdot}7 \times 10^{-4}$ and $1{\cdot}3 \times 10^{-3}$ m/day were obtained for the crust and soft clay respectively. Subsequently studies showed that satisfactory matching with the A403 field data could be obtained using a single value of initial horizontal permeability k_h of 10^{-3} m/day, and this has been used for the analysis reported here. A ratio of horizontal to vertical permeability $k_h/k_z = 1{\cdot}5$ was assumed, which probably underestimates the conditions in the field. The permeabilities of the smear zone were reduced by a factor of 2·5 within a radius equal to twice the drain radius, although there was uncertainty over whether to base the size of the smear zone on the drain size or that of the mandrel (Holtz *et al.*, 1991). In all analyses nodal coordinates and permeability were continuously updated as the analysis progressed.

The vertical drain, surface granular layer and underlying terrace gravel all provide free drainage, and with the piezometric level in the gravel set at 7 m below ground level, the boundary conditions are affected by the under-drainage. Although it might be expected that, with the installation of vertical drains, final piezometric levels in the soft clay would be

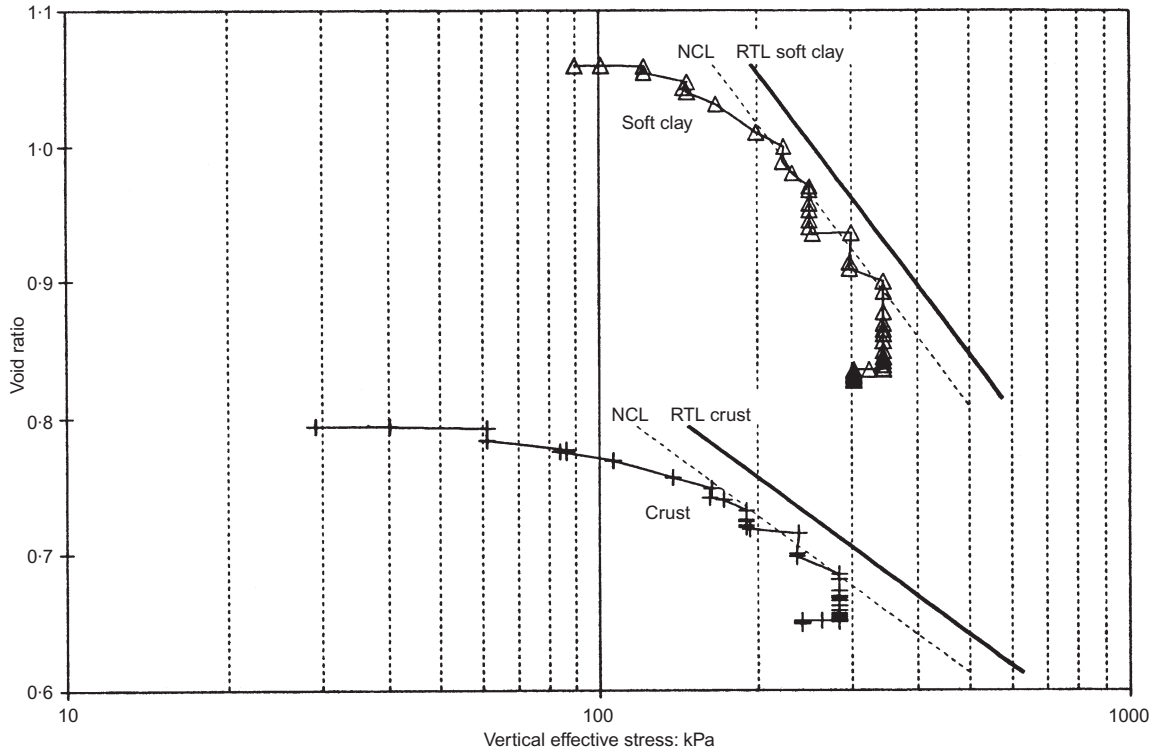

Fig. 10. Field observations of void ratio against effective stress for crust and soft clay layers, and reference time lines used in analysis

Table 2. Soil parameters for A403 embankment derived from back-analysis of extensometer data

Layer	Depth: m	m_v: m^2/kN	e_0	λ	κ	ψ	$\sigma_0'^{ep}$	ε_0^{ep}	t_0: days
Crust	0–3		0·794	0·125	0·018	0·0117	148	0	0·5
Soft silty clay	3–7		1·060	0·227	0·027	0·0239	195	0	2·0
Silty sand	7–11	$6{\cdot}8 \times 10^{-5}$							

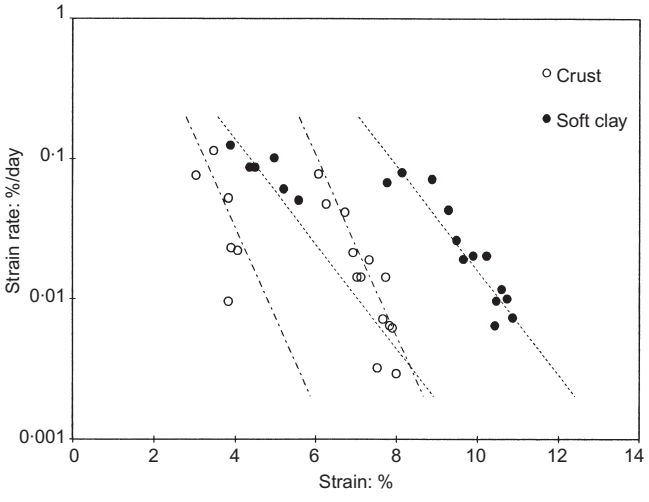

Fig. 11. Variation of strain rate with strain during two creep periods for crust and soft clay layers

lower than the initial ones, there was no field evidence for this. Accordingly it was decided to assume that initial and final pore pressure distributions would be similar, with zero pore pressure specified in the strata located initially above the piezometric level in the gravel. The analyses were therefore carried out using the original version of BRISCON, in which *excess* pore pressure is the dependent variable.

Before attempting to model the whole construction sequence, BRISCON was used to check that the creep behaviour of each layer could be predicted. Using the parameters in Table 2 the behaviour during the two rest periods was predicted, and Fig. 12 shows that a good matching of the magnitude and rates of compression was achieved.

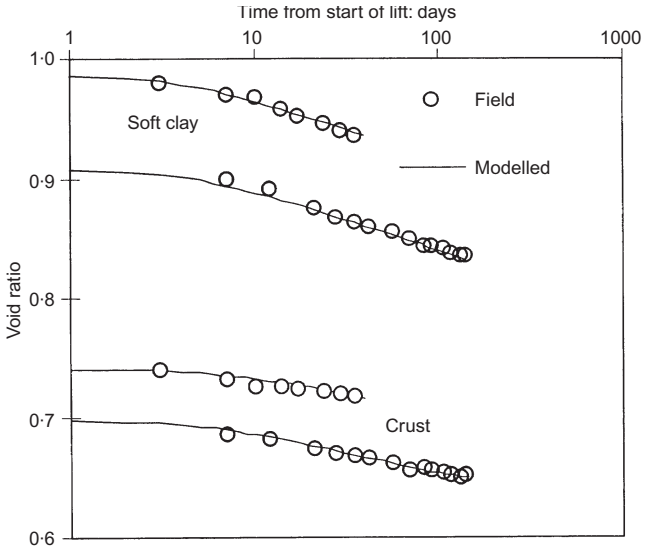

Fig. 12. Comparison of behaviour predicted with BRISCON with observed creep during two rest periods for soft clay layer and overlying crust

Finally the behaviour of the whole profile subjected to the field construction sequence was modelled using an initial horizontal permeability of 10^{-3} m/day As shown in Fig. 13(a), the whole time–settlement history could be predicted satisfactorily. The predicted excess pore pressures for a soil element near the top of the soft clay just below the crust are compared with the field data in Fig. 13(b), and it may be seen that they are underpredicted by a factor of 3. Although the difference may appear large it does not significantly affect the effective stress in the ground since the absolute pore pressures are small. The influence of permeability on the predicted excess pore pressures is discussed further in the next section. The predicted change of state of a soil element near the top of the soft clay layer has been compared with that deduced from the field instrumentation in Fig. 14. Here the void ratio and effective stress predicted by BRISCON may be seen to match well with data re-plotted from Fig. 10.

These analyses also show that the 2 m surcharge was not

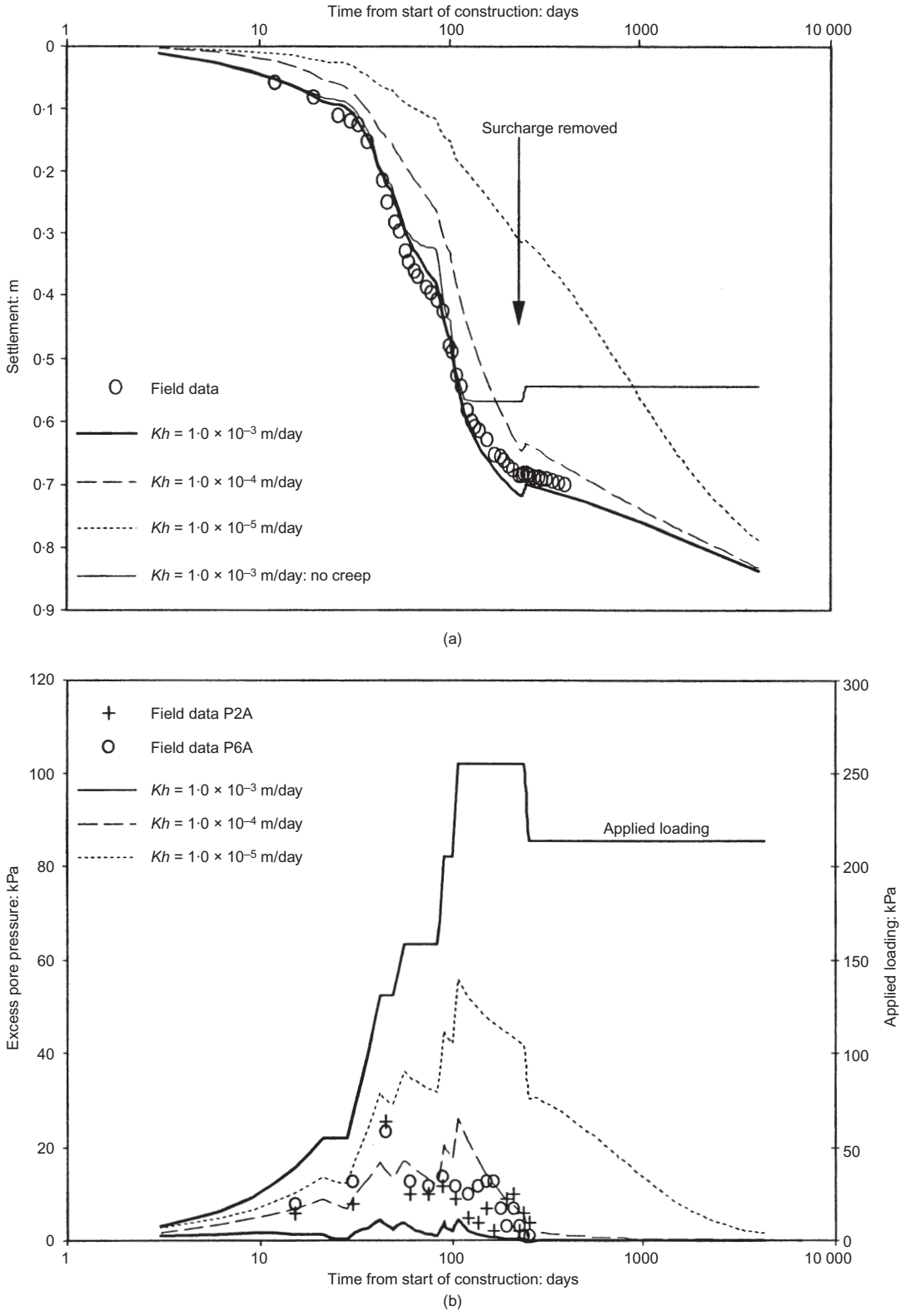

Fig. 13. Comparison between observed and predicted settlement and excess pore pressures at A403 overbridge embankment

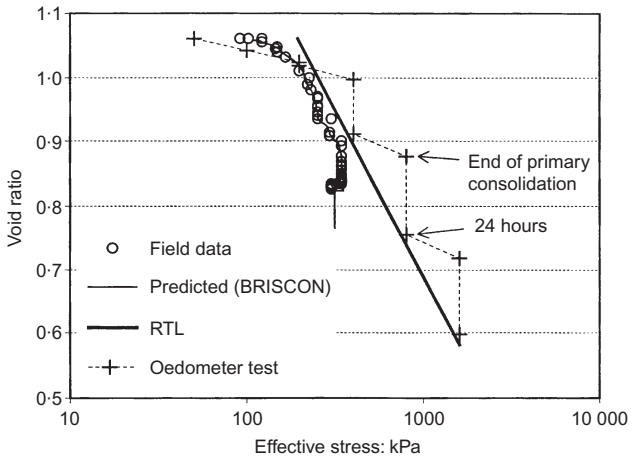

Fig. 14. Observed and predicted behaviour of soft clay in the field, and predicted behaviour in an oedometer test

sufficient to eliminate post-construction settlement. Indeed, it is predicted that in the long term the settlement will increase by a further 15 cm over 50 years. By extending the parametric study to examine the effectiveness of surcharge it was shown (Nash & Ryde, 1999) that at least 4 m surcharge would have been needed for the 5-month surcharge period to reduce the post-construction settlement by 50%.

Further analyses

On account of the uncertainty over the values of permeability, a parametric study was carried out in which the initial permeabilities (k_h of 10^{-3}m/day, $k_h/k_z = 1{\cdot}5$) were reduced by factors of 10 and 100. The predicted settlement behaviour is presented in Fig. 13(a), which shows that while a tenfold reduction of permeability has little effect, a hundredfold reduction significantly slows the consolidation. Examination of the predicted excess pore pressures shown in Fig. 13(b) indicates that, as expected, larger excess pore pressures develop when the permeability is reduced. These analyses suggest that for the best matching of settlement and excess pore pressure data, an initial average horizontal permeability of these soft silty soils of about 3×10^{-4} m/day should be used. With such a heterogeneous estuarine deposit, in which flow may be concentrated in the more permeable laminations, a single value of permeability can only represent an equivalent average value. Indeed, the predicted excess pore pressures are also sensitive to the assumed effective drain size, and the permeability and extent of the smear zone.

Additional analyses were carried out to explore aspects of the creep behaviour. First the behaviour in a conventional oedometer test on the soft clay was predicted, using the parameters given in Table 2, with loading increased every 24 hours with a load increment ratio of 2. The void ratio against effective stress behaviour is shown alongside the full-scale behaviour and RTL in Fig. 14. As might be expected for very short drainage paths, the laboratory strain rates are much higher than those in the field, and at higher stresses the void ratio lies above the RTL. Using this constitutive model, the soil state at end of primary consolidation (EOP) in the laboratory is quite different from that in the field, as was shown by Fig. 2 and discussed earlier in the paper.

Second, an analysis was carried out to explore the significance of not modelling creep. This was carried out using the field normal consolidation lines (NCL shown dashed in Fig. 10) to define the stress–strain behaviour. The results are presented in Fig. 13(a) alongside those using the creep model, and indicate very similar behaviour up to maximum load, but thereafter there is of course no further movement. The behaviour up to the end of primary consolidation is similar to that predicted with the EVP model since the chosen NCL coincides with the field NCL, which was well matched by the analysis with the creep model. To predict the long-term behaviour it would be necessary to add secondary consolidation in a conventional way with the usual difficulties of defining the time origin. If the modelled permeability had been lower, or if the location of the NCL had been higher (e.g. end-of-primary or 24-hour lines from oedometer tests indicated in Fig. 14), the analysis without creep would have underestimated the settlement at all stages.

DISCUSSION AND CONCLUSION

The consolidation of soft soils accelerated by vertical drains frequently presents difficulties to designers of embankments and reclamation schemes over soft clays if there is significant creep. The elastic visco-plastic constitutive model developed originally by Yin & Graham (1989, 1996) reproduces many features of soft clay behaviour commonly observed in the field and laboratory, and provides a helpful framework for the interpretation of data from high-quality oedometer tests and field instrumentation. It is axiomatic that the field and laboratory stress–strain paths predicted by the model are different on account of the longer drainage paths and slower strain rates in the field. The incorpation of this EVP model in the finite difference procedure BRISCON enables predictions to be made for full-scale problems. Parametric studies may be undertaken where there is uncertainty over soil properties such as permeability and creep parameters, and to examine the effects of varying the size and permeability of the smear zone and the effects of drain resistance.

The case study presented here has illustrated the application of the model to the analysis of a full-scale problem involving significant creep; its use in back-analysis of field consolidation behaviour is believed to be novel. The derivation of the creep parameters from the field instrumentation data was facilitated by the rapid dissipation of excess pore pressures so that there were significant periods of drained creep during construction. If pore pressures had not dissipated so rapidly a more complicated procedure would have been required on account of the continuous variation of effective stress. While BRISCON could predict the field settlement behaviour and rapid pore pressure dissipation at the A403 overbridge satisfactorily, its application to a future project where there are high-quality laboratory data is necessary to test its validity during primary consolidation.

A significant aspect of the EVP model is that the creep strain rate depends only on the current state of the soil. This enables predictions to be made of behaviour after removal of a surcharge without resorting to empirical methods. While simple hand calculations may be made to assess surcharge effectiveness where primary consolidation occurs quickly (Nash & Ryde, 1999), the BRISCON procedure facilitates design to reduce long-term secondary settlements even if primary consolidation is not complete before a surcharge is removed.

The satisfactory comparison of analyses of simple axisymmetric problems using BRISCON with analyses using CRISP suggests that the assumption of one-dimensional strains in the former may not result in significant inaccuracy. This supports the use of a one-dimensional procedure when analysing conditions near the centre-line of embankments, and of course for one-dimensional problems such as reclamations. Where significant shear strains may occur, a more comprehensive analysis is required using procedures such as those developed by Hird *et al.* (1992), in which the vertical drains are incorporated into a full two-dimensional finite element model. However, such analyses have not hitherto used a constitutive model incorporating creep, and would necessitate using a more comprehensive model such as that developed recently by Yin & Graham (1999).

ACKNOWLEDGEMENTS

The authors are grateful to the Second Severn Crossing Group for access to the field data, to them and the Engineering and Physical Sciences Research Council for sponsoring the research, and to Prof David Muir Wood for his helpful comments on the manuscript.

APPENDIX 1. DERIVATION OF THE BOUNDARY PERMEABILITY VALUES k_X

An equivalent value of permeability, k_X, is needed for use in the finite difference equation (9) when determining the hydraulic gradient at a cell boundary between two soils of different permeability. Fig. 15 shows point X on a boundary between adjacent nodes M and N in layers of permeability k_m and k_n. The total head differences between the various points are given by Δh_{mx} and Δh_{nx}. Considering the continuity of flow across the boundary, the discharge velocity V perpendicular to the boundary at all three points must be equal, and is given by

$$V = \frac{k_m \Delta h_{mx}}{L_m} = \frac{k_n \Delta h_{nx}}{L_n} = k_X \frac{\Delta h_{mx} + \Delta h_{nx}}{L_m + L_n} \tag{15}$$

Since the boundary is midway between the nodes $L_m = L_n$, and equation (15) may be rearranged to show that;

$$k_X = \frac{2k_m k_n}{k_m + k_n} \tag{16}$$

This equation may be used without modification at the grid boundaries to ensure that the correct boundary conditions are implemented. At an impermeable boundary between cells M and N, use of $k_m = 0$ leads to $k_X = 0$, ensuring that the discharge velocity is zero. At a permeable boundary the pore pressure or total head is specified at the phantom node outside the grid, and the use of $k_m = \infty$ leads to the equivalent boundary permeability $k_X = 2k_n$ for use in equation (11).

NOTATION

c_v, c_r	vertical and radial coefficients of consolidation $k_z/\gamma_w m_v$, $k_r/\gamma_w m_v$
C_α	logarithmic creep function with respect to void ratio
C_c	compression index
e	void ratio
k_z, k_h, k_r	vertical, horizontal and radial coefficients of (here $k_h = k$) permeability
k_T, k_B, k_I, k	coefficients of permeability at cell boundaries
m_v	coefficient of elastic volume compressibility
t, t_e	time and equivalent time
t_0	parameter used to determine strain rate on reference time line
u, $\bar{u}$, u_{ss}	pore pressure, excess pore pressure, steady-state pore pressure
u^*	pore pressure used for prediction of pore pressure at end of time step
v, v_0	specific volume, specific volume at zero strain
γ_w	unit weight of water
ε	strain
σ, σ'	vertical total and effective stresses
σ'_0, ε_0	values of effective stress and strain for fixing reference time line
κ, λ	logarithmic material parameters for elastic and stress-dependent plastic strains
ψ	logarithmic material parameter for creep

Superscripts and subscripts

e, ep, tp	instantaneous (elastic), stress-dependent plastic and time-dependent plastic
i, j	counters for radial and vertical position on grid

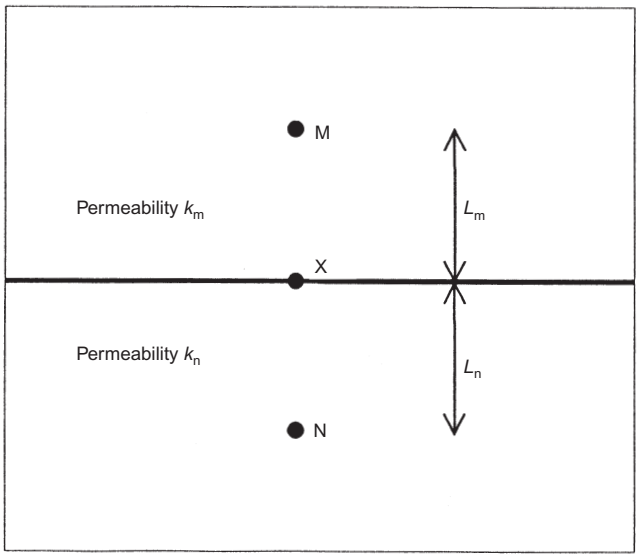

Fig. 15. Part of finite difference grid showing boundary between soils of different permeability

REFERENCES

Barron, R. A. (1948). Consolidation of fine-grained soils by drain wells. *Trans. ASCE* **113**, 718–754.

Berre, T. & Iversen, K. (1972). Oedometer tests with different specimen heights on a clay exhibiting large secondary compression. *Géotechnique* **22**, No. 1, 53–70.

Bjerrum, L. (1967). Engineering geology of Norwegian normally consolidated clays. Seventh Rankine Lecture. *Géotechnique* **17**, No. 2, 81–118.

Bjerrum, L. (1972). Embankments on soft ground. State of the art report. *Proceedings of the special conference on performance of earth and earth-supported structures*, Purdue University, Vol. 1, pp. 1–54. ASCE.

Butterfield, R. (1979). A natural compression law for soils (an advance on e–log p'). *Géotechnique* **29**, No. 4, 469–480.

Carrillo, N. (1942). Simple two- and three-dimensional cases in the theory of consolidation of soils. *J. Maths. Physics* **21**, No. 1, 1–15.

Cook, D. A. & Pereira, G. (1991). Records of settlement of the M5 motorway over the Somerset levels. In *Quarternary engineering geology*, Engineering Geology Spec. Pub. No. 7, pp. 627–635. London: Geological Society.

Crank, J. & Nicolson, P. (1947). A practical method for numerical evaluation of solutions of partial differential equations. *Proc. Camb. Phil. Soc.* **43**, 50–67.

Den Haan, E. J. (1992). The formulation of virgin compression in soils. *Géotechnique* **42**, No. 3, 465–484.

Den Haan, E. J. (1996). A compression model for non-brittle soft clays and peat. *Géotechnique* **46**, No. 1, 1–16.

Garlanger, J. E. (1972). Consolidation of soils exhibiting creep under constant effective stress. *Géotechnique* **22**, No. 1, 71–78.

Hansbo, S. (1981). Consolidation of fine-grained soils by prefabricated drains. *Proc. 10th Conf. on SMFE, Stockholm* **3**, 677–682.

Hird, C. C., Pyrah, I. C. & Russell, D. (1992). Finite element modelling of vertical drains beneath embankments on soft ground. *Géotechnique* **42**, No. 3, 499–511.

Holtz, R. D., Jamiolkowski, M., Lancellotta, R. & Pedroni, R. (1991). *Prefabricated vertical drains: design and performance*, CIRIA Ground Engineering Report: Ground Improvement. Oxford: Butterworth-Heinemann.

Jamiolkowski, M., Lancellotta, R. & Wolski, W. (1983). Precompression and speeding up consolidation, General Report to Spec. Session 6. *Proc. 8th Eur. conf. on SMFE, Helsinki* **3**, 1201–1226.

Johnson, S. J. (1970). Precompression for improving foundation soils. *J. Soil Mech. and Found. Div., ASCE* **96**, No. SM1, 111–144.

Kabbaj, M., Oka, F., Leroueil, S. & Tavenas, F. (1986). Consolidation of natural clays and laboratory testing. In *Consolidation of soils: testing and evaluation* (eds R. N. Yong and F. C. Townsend), ASTM STP 892, 71–103.

Ladd, C. C., Foott, R., Ishihara, K., Schlosser, F. & Poulos, H. G. (1976). Stress-deformation and strength characteristics: state-of-the-art report. *Proc. 9th Int. Conf. on SMFE, Tokyo* **2**, 421–494.

Lambe, T. W. (1973). Predictions in soil engineering. *Géotechnique* **23**, No. 2, 149–202.

Lee, I. K., White, W. & Ingles, O. G. (1983). *Geotechnical engineering*. Boston, Mass Pitman.

Leroueil, S. (1988). Recent developments in consolidation of natural clays. 10th Canadian Geotechnical Colloquium. *Can. Geotech. J.* **25**, No. 1, 85–107.

Magnan, J.-P., Baghery, S., Brucy, M. & Tavenas, F. (1979). Etude numérique de la consolidation unidimensionnelle en tenant compte des variations de la perméabilité et de la compressibilité du sol, du fluage et de la non-saturation. *Bull. Liaison Lab. Ponts et Chaussées* **103**, 83–94.

Mesri, G. & Choi, Y. K. (1985a). The uniqueness of the end-of-primary (EOP) void ratio-effective stress relationship. *Proc. 11th Int. Conf. on SMFE, San Francisco* **2**, 587–590.

Mesri, G. & Choi, Y. K. (1985b). Settlement analysis of embankments on soft calys. *J. Geotech. Engng Div., ASCE* **111**, No. GT4, 441–464.

Mesri, G. & Godlewski, P. M. (1977). Time- and stress-compressibility interrelationship. *J. Geotech. Engng Div., ASCE* **103**, No. GT5, 417–429.

Mesri, G. & Rokhsar, A. (1974). Theory of consolidation for clays. *J. Geotech. Engng Div., ASCE* **100**, No. GT8, 889–904.

Mesri, G., Lo, D. O. K. & Feng, T. W. (1994). Settlement of embankments on soft clays. In *Vertical and horizontal deformations of foundations and embankments*, ASCE. Geot. Spec. Pub. No. 40, pp. 8–55.

Morton, K. W. & Mayers, D. F. (1994). *Numerical solution of partial differential equations*. Cambridge: Cambridge University Press.

Murray, R. T. (1971). *Embankments constructed on soft foundations: settlement study at Avonmouth*, Report LR 419. Crowthorne: Road Research Laboratory.

Nash, D. F. T. & Ryde, S. J. (1999). Modelling the effects of surcharge to reduce long term settlement of an embankment on soft alluvium. In *Geotechnical Engineering for Transporation Infrastructre: Proc. 12th Eur. Conf. on SMGE, Amsterdam* **3**, 1555–1561. Rotterdam: Balkema.

Nash, D. F. T & Ryde, S. J. (2000). Modelling the effects of surcharge to reduce long term settlement of reclamations over soft clays. *Proceedings of the international symposium on coastal geotechnical engineering in practice*, **I**, 483–480 Yokahama. Rotterdam: Balkema.

Olsen, R. E. & Ladd, C. C. (1979). One-dimensional consolidation problems. *J. Geotech. Eng Div., ASCE* **105**, No. GT1, 11–30.

Olsen, R. E., Daniel, D. E. & Liu, T. K. (1974). Finite difference analysis for sand drain problems. *Proceedings of the conference on analysis and design in geotechnical engineering*, Vol. 1, pp. 85–110. ASCE.

Onoue, A. (1988). Consolidation of multi-layered anisotropic soils by vertical drains with well resistance. *Soils Found.* **28**, No. 3, 75–90.

Reece, G. (1986). *Microcomputer modelling by finite differences*. London: Macmillan.

Richart, F. E. (1959). Review of the theories for sand drains. *Trans. ASCE* **124**, 709–739.

Ryde, S. J. (1997). *The performance and back-analysis of embankments on soft estuarine clay.* PhD thesis, University of Bristol.

Suklje, L. (1957). The analysis of the consolidation process by the isotache method. *Proc. 4th Int. Conf. on SMFE* **1**, 200–206.

Taylor, D. W. (1948). *Fundamentals of soil mechanics*. London: Chapman & Hall; New York: Wiley.

Taylor, D. W. & Merchant, W. (1940). A theory of clay consolidation accounting for secondary compression. *J. Math. Phys.* **19**, No. 3, 167–185.

Terzaghi, K. (1943). *Theoretical soil mechanics*. London : Chapman & Hall; New York: Wiley.

Terzaghi, K. & Peck, R. B. (1948). *Soil mechanics in engineering practice*. London: Chapman & Hall; New York: Wiley.

Yin, J.-H. & Graham, J. (1989). Viscous-elastic-plastic modelling of one-dimensional time-dependent behaviour. *Can. Geotech. J.* **26**, No. 2, 199–209.

Yin, J.-H. & Graham, J. (1994). Equivalent times and one-dimensional elastic visco-plastic modelling of time-dependent stress–strain behaviour of clays. *Can. Geotech. J.* **31**, No. 1, 42–52.

Yin, J.-H. & Graham, J. (1996). Elastic visco-plastic modelling of one-dimensional consolidation. *Géotechnique* **46**, No. 3, 515–527.

Yin, J.-H. & Graham, J. (1999). Elastic viscoplastic modelling of the time-dependent stress–strain behaviour of soils. *Can. Geotech. J.* **36**, No. 4, 736–745.